SUB-PIXEL TARGET SPECTRA ESTIMATION AND DETECTION USING FUNCTIONS OF MULTIPLE INSTANCES

Alina Zare[*], *Paul Gader*[†], *Jeremy Bolton*[†], *Seniha Yuksel*[†], *Thierry Dubroca*[+], *Ryan Close*[†], *Rolf Hummel*[+]

[*]Electrical and Computer Engineering, University of Missouri
[†]Computer and Information Science and Engineering, University of Florida
[+]Material Science and Engineering, University of Florida

ABSTRACT

The Functions of Multiple Instances (FUMI) method for learning target pattern and non-target patterns is introduced and extended. The FUMI method differs significantly from traditional supervised learning algorithms because only functions of target patterns are available. Moreover, these functions are likely to involve other non-target patterns. In this paper, data points which are convex combinations of a target prototype and several non-target prototypes are considered. The Convex-FUMI (C-FUMI) method learns the target and non-target patterns, the number of non-target patterns, and the weights (or proportions) of all the prototypes for each data point. For hyperspectral image analysis, the target and non-target prototypes estimated using C-FUMI are the endmembers for the target material and non-target (background) materials. For this method, training data need only binary labels indicating whether a data point contains or does not contain some proportion of the target endmember; the specific target proportions for the training data are not needed. In this paper, the C-FUMI algorithm is extended to incorporate weights for training data such that target and non-target training data sets are balanced (resulting in the Weighted C-FUMI algorithm). After learning the target prototype using the binary-labeled training data, target detection is performed on test data. Results showing sub-pixel explosives detection and sub-pixel target detection on simulated data are presented.

1. INTRODUCTION

The FUMI algorithm is a generalization of Multiple Instance Learning (MIL) methods [1, 2, 3, 4, 5, 6]. In MIL, training data are divided into positive and negative "bags." A bag is defined to be a multi-set of data points. A positive bag includes at least one target point. In each positive bag, the exact number of data points belonging to the target class is unknown. Negative bags are composed entirely of non-target data points. The MIL methods are effective for learning target concepts and developing classifiers for cases where accurate sample-level labeled training data is unavailable.

The FUMI method can be related to the MIL framework by treating each data point as being a function of a positive or negative bag. FUMI learns target and non-target prototypes given a set of data points that are some unknown function of the target and non-target prototypes. Suppose there is a given data set $\mathbf{X} = \{\mathbf{x}_1, \mathbf{x}_2, ..., \mathbf{x}_N\}$ where each data point is some unknown function of prototypes, $\mathbf{x}_i = f(\mathbf{B}_i, \mathbf{P}_i)$ where $\mathbf{P}_i$ are the set of parameters for $\mathbf{x}_i$ and $\mathbf{B}_i$ is the "bag" of prototypes that contribute in a non-negligible way to the data point $\mathbf{x}_i$. Each training point $\mathbf{x}_i$ is given a binary label $l(\mathbf{x}_i)$ where $l(\mathbf{x}_i) = 1$ if $\mathbf{b}_T \in \mathbf{B}_i$ and $l(\mathbf{x}_i) = 0$ if $\mathbf{b}_T \notin \mathbf{B}_i$. After learning the target prototype using the binary-labeled training data, target detection can be performed on test data using the following method.

In this paper, the specific case that is considered is that each data point is assumed to be a convex combination of target and non-target prototypes, as shown in Equation 1 where the set of prototypes, $\mathbf{E}$, with non-zero weights for data points $\mathbf{x}_i$ define the bag $\mathbf{B}_i$.

$$\mathbf{x}_i = p_{iT}\mathbf{e}_T + \sum_{k=1}^{M} p_{ik}\mathbf{e}_k \tag{1}$$

where $\mathbf{x}_i$ is a data point, $\mathbf{e}_T$ is the target prototype, $\mathbf{e}_k$ is a non-target prototype for $k = 1, ..., M$ and p_{ik} is the weight (or proportion value) of the k^{th} prototype in data point i. The proportions are constrained to sum-to-one and be greater than zero.

$$p_{iT} + \sum_{k=1}^{M} p_{ik} = 1, \quad p_{iT} \geq 0, \quad p_{ik} \geq 0 \tag{2}$$

Endmember detection and spectral unmixing are common tasks in hyperspectral image (HSI) analysis [7]. Given an HSI analysis task, the target and non-target prototypes estimated using C-FUMI are the target and background endmembers.

If $l(\mathbf{x}_i) = 1$ then $\mathbf{x}_i = p_{iT}\mathbf{e}_T + \sum_{k=1}^{M} p_{ik}\mathbf{e}_k$ with $p_{iT} > 0$. If $l(\mathbf{x}_i) = 0$, then $\mathbf{x}_i = \sum_{k=1}^{M} p_{ik}\mathbf{e}_k$. The exact proportion values for the training data are not needed. Therefore, C-FUMI [8] learns the spectral shape of a target endmember given mixed training data without prior knowledge of the proportions of the target in each positively-labeled training point.

978-1-4577-2201-1/11/$26.00 ©2011 IEEE

In the following section, the Weighted C-FUMI algorithm is developed. In addition to learning prototypes, the Weighted C-FUMI algorithm learns the number of non-target endmembers needed for a data set and determines the proportions of endmembers for each data point. Experimental results, discussion and future work sections are found in Sections 3 and 4.

2. THE WEIGHTED C-FUMI ALGORITHM

The Weighted C-FUMI Algorithm is an extension of the C-FUMI algorithm [8] which is, in turn, an extension of the Sparsity Promoting Iterated Constrained Endmembers (SPICE) algorithm [7]. In SPICE, endmembers and proportions are iteratively updated by minimizing the objective function in Equation 3 where $\gamma_k = \frac{\Gamma}{\sum_{i=1}^{N} p_{ik}}$ using the proportions from the previous iteration and Γ is a parameter used to control the degree of sparsity. The first term of this objective computes the squared error between the input data and the estimate found using the current prototypes (or *endmembers*) and proportions. The second term produces endmembers that provide a tight fit around the data. The third term is a sparsity promoting term used to determine M, the number of endmembers needed to describe the input data. This objective is updated iteratively using alternating optimization on the endmembers and proportions.

The SPICE algorithm is an unsupervised algorithm to learn the proportions, the endmembers, and the number of endmembers, M, for a given unlabeled dataset. The Weighted C-FUMI (and C-FUMI) algorithm extends the SPICE algorithm by using the labeled training points to learn and distinguish the specific target endmembers from the remaining non-target background endmembers. The target endmembers found can then be used for detection in test data. The Weighted C-FUMI algorithm extends C-FUMI by incorporating weights in the first term of the objective function to balance target and non-target training sets. Often, there are many more non-target training pixels than target training pixels, to emphasize the target training data a weight is placed on their error terms in the objective function to enhance their contribution to the estimate of the target and background endmembers.

For negatively labeled training data, the proportion value associated with the target prototype is constrained to be zero. Therefore, the objective function for Weighted C-FUMI can be written as shown in Equation 4. The value for $w_{l(\mathbf{x}_i)} = l(\mathbf{x}_i)\left(\frac{\alpha N_n}{N_t}\right)$ where N_n and N_t are the number of samples with $l(\mathbf{x}_i) = 0$ and $l(\mathbf{x}_i) = 1$, respectively. Therefore, if the parameter α is set to 1, then the weight on the target points is scaled such that the collection of target points has the same influence on the first term as the collection of non-target training points. Furthermore, α can be set to larger than 1 to emphasize the importance of target training data over background data.

The Weighted C-FUMI algorithm updates the target and non-target endmembers, proportions, and number of endmembers by iteratively minimizing the objective function in Equation 4. In order to update both target and non-target endmembers, the proportions for all data points are held constant and Equation 4 is minimized by setting the derivative of the objective with respect to each endmember to zero and solving for the endmember value. When updating proportions, endmembers are held constant and Equation 4 is minimized subject to the constraints in Equation 2. Since this is a quadratic objective with linear constraints, a quadratic programming step is used to update the proportions. The sparsity promoting term (the 4^{th} term in the objective) is used to determine the number of non-target endmembers needed. This term drives the proportions associated with unneeded non-target endmembers to zero. Then, the unneeded endmembers can be removed with no effect on the squared error terms. The objective function is iteratively minimized until some stopping criterion is reached such as convergence or a maximum number of iterations.

After learning target and non-target prototypes, target detection on test data can be carried out. Given the prototypes and test data, the proportions for all the prototypes for the given test data are computed by minimizing the residual sum of squared errors, $\left|\left|\left(\mathbf{x}_i - p_{iT}\mathbf{e}_T - \sum_{k=1}^{M} p_{ik}\mathbf{e}_k\right)\right|\right|_2^2$ subject to the constraints in Equation 2 using a quadratic programming step. The proportion value for the target endmember is used as the detection statistic.

3. EXPERIMENTAL RESULTS

Two experiments were performed. The first was performed with real hyperspectral data for explosives detection and the other with synthetic data. The latter data set was used to investigate accuracy and produced some interesting results for further investigation. The first experiment was applied to differential reflectometry hyperspectral data (with 512 spectral bands ranging from 100 to 612 nm in wavelength) [9, 10] for explosives detection. Figure 1 shows an example of the area scanned by the differential reflectometer. Two data collections were conducted in which several spectra were collected both with and without explosive material. The first run was used as training data to estimate the target and background endmembers and, then, the second run was used for testing where the data was unmixed using the estimated target and background endmembers. For training, target and non-target spectra were identified by hand and assigned positive or negative labels. A "buffer" zone around the explosive material was identified in the training and testing data in which the pixels were not labeled target nor non-target to account for any uncertainty in spectral collection locations. Weighted C-FUMI was applied with the following parameter settings:

$$G = (1-\mu)\sum_{i=1}^{N}\left|\left|\left(\mathbf{x}_i - \sum_{k=1}^{M} p_{ik}\mathbf{e}_k\right)\right|\right|_2^2 + \frac{\mu}{2}\sum_{k=1}^{M}\sum_{j=1}^{M}||(\mathbf{e}_k - \mathbf{e}_j)||_2^2 + \sum_{k=1}^{M}\gamma_k\sum_{i=1}^{N}p_{ik} \tag{3}$$

$$F = (1-\mu)\sum_{i=1}^{N} w_{l(\mathbf{x}_i)}\left|\left|\left(\mathbf{x}_i - l(\mathbf{x}_i)p_{iT}\mathbf{e}_T - \sum_{k=1}^{M} p_{ik}\mathbf{e}_k\right)\right|\right|_2^2 + \frac{\mu}{2}\sum_{k=1}^{M}\sum_{j=1}^{M}||(\mathbf{e}_k - \mathbf{e}_j)||_2^2 + \mu\sum_{k=1}^{M}||(\mathbf{e}_T - \mathbf{e}_k)||_2^2 + \sum_{k=1}^{M}\gamma_k\sum_{i=1}^{N}p_{ik} \tag{4}$$

$\mu = 1 \times 10^{-4}$, $\Gamma = 2$, $M = 9$, and $\alpha = 2$. After learning the endmembers, the proportions for every data point in the test data were computed; the proportion values on the target endmember were compared to the labels for test data. Figure 2 shows the endmembers found by the Weighted C-FUMI algorithm. Figure 3 shows histograms of proportions estimated by Weighted C-FUMI on the target and non-target test data for the target endmember. Using a threshold value of 0.4, classification of all pixels containing explosive material are correctly identified as containing target and none of the background pixels are incorrectly identified.

Fig. 1. Distribution of explosive material on cloth background. The black background to the side (and underneath) the red cloth is a carbon-pad. The cloth is thin and the carbon-pad can be easily seen through the cloth. The explosive material is unevenly distributed on the cloth and, thus, the cloth can often be seen through the explosive material. On either side of the explosive material is pink Polytetrafluoroethylene tape.

Weighted C-FUMI was run on simulated data to estimate the capabilities of accurately detecting sub-pixel targets generated using random mixtures of three prototypes. The prototypes used were selected from the ASTER spectral library. Specifically, the Borate, Carbonate Burkeic, Chloride, and Sulfate Anhydric spectra. Borate was labeled the target spectrum. Training data containing 50 target and 99 non-target points were generated. The 50 target points were created by generating mixtures of the four endmembers, including the target endmember. The 99 non-target points were generated using mixtures of the three non-target endmembers. Mixtures were generated by drawing proportion values from Dirichlet distributions with varying parameter values. Nine experiments were conducted in which the Dirichlet parameters used

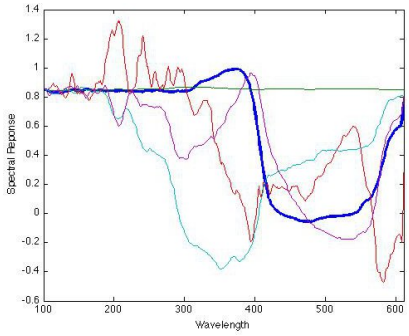

Fig. 2. Endmembers found using Weighted C-FUMI. Target endmember is shown in bolded dark blue. It is a good representative of known TNT (target material) signatures [10].

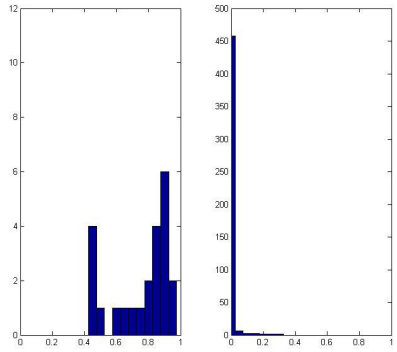

Fig. 3. Histograms of proportions estimated on test data for the explosive material on (a - left) target and (b - right) non-target test pixels. Using a threshold value of 0.4 for the target proportion value, all target pixels can be correctly identified without false alarms on the non-target test pixels.

to the draw the proportions for the target endmembers were set to: (0.9, 0.025, 0.05, 0.025), (0.8, 0.1, 0.5, 0.5), (0.7, 0.15, 0.1, 0.05), (0.6, 0.1, 0.2, 0.1), (0.5, 0.2, 0.2, 0.1), (0.4, 0.3, 0.15, 0.15), (0.3, 0.7, 0, 0), (0.2, 0.4, 0.3, 0.1), and (0.1, 0.1, 0.1, 0.7), respectively. The Dirichlet parameters for the three groups of background endmembers were set to (0 0.01 0.01 0.98), (0 0.05 0.9 0.05), and (0 0.8 0.1 0.1), respectively, where the first value is the proportion on the target endmember and the next three value are the average proportion for

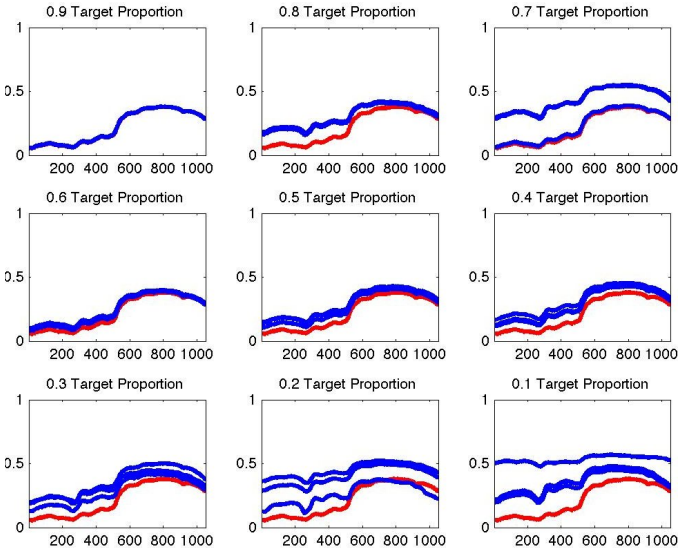

Fig. 4. Comparison of true and estimated target endmembers found using the Weighted C-FUMI algorithm with target proportions on the test pixels beginning at 0.9 and decreasing to 0.1 in nine experiments with 3 random intitializations. X-axis is band number. Y-axis is normalized spectral response. Experiments ranged from easy to extremely difficult (where the target proportions for all the target pixels were close to a value of only 0.1). All experiments contained 4 endmembers one of which was the target endmember. The estimate for the target endmember from 3 runs is shown in blue. The true target spectrum is shown in red. In 1st and 3rd plot, the estimated endmember matches the true endmember extremely closely and, thus, masks the true endmember spectral plot.

the background endmembers. Weighted C-FUMI was applied to this training data with the following parameter settings: $\mu = 1 \times 10^{-4}$, $\Gamma = 2$, $M = 9$, and $\alpha = 2$. The true and estimated target endmembers for the range of target proportion values in the training data are shown in Figure 4. Each experiment was run multiple times; the figure displays the results of three runs with randomly generated data (ranging in difficulty) and random initialization. As can be seen, the target endmember is closely approximated.

4. CONCLUSION AND FUTURE WORK

We are currently running additional experiments to detect explosives on varying background materials. Currently, a single target endmember is found, current work includes detecting multiple target materials. In many datasets, pixels are often associated with a small number of endmembers. Sparsity promoting priors can be incorporated to encourage each data point to have non-zero proportions associated with a small number of endmembers. Also, for image data, spatial information may be incorporated to help improve results. Finally, investigations into methods to have the target endmember have as unique of a spectral shape from background endmembers as possible are being conducted. Non-linear methods will also be investigated.

5. REFERENCES

[1] T. G. Dietterich, R. H. Lathrop, and T. Lozano-Perez, "Solving the multiple-instance problem with axis-parallel rectangles," *Artificial Intelligence*, vol. 89, no. 1-2, pp. 31–17, 1997.

[2] O. Maron and T. Lozano-Perez, "A framework for multiple-instance learning.," *Neural Information Processing Systems*, vol. 10, 1998.

[3] J. Bolton and P. Gader, "Multiple Instance Learning for Hyperspectral Image Analysis," *IEEE International Geoscience and Remote Sensing Symposium*, 2010, (In Press).

[4] Jeremy Bolton, Paul Gader, Hichem Frigui, and Pete Torrione, "Random set framework for multiple instance learning," *Information Sciences*, vol. In Press, Corrected Proof, pp. –, 2011.

[5] V.C. Raykar, B. Krishnapuram, J. Bi, M. Dundar, and R.B. Rao, "Bayesian multiple instance learning: automatic feature selection and inductive transfer," in *Proceedings of the 25th international conference on Machine learning*. ACM New York, NY, USA, 2008, pp. 808–815.

[6] Q. Zhang and S.A. Goldman, "EM-DD: An improved multiple-instance learning technique," *Advances in Neural Information Processing Systems*, vol. 2, pp. 1073–1080, 2002.

[7] A. Zare and P. Gader, "Sparsity promoting iterated constrained endmember detection for hyperspectral imagery," *IEEE Geoscience and Remote Sensing Letters*, vol. 4, no. 3, pp. 446–450, July 2007.

[8] A. Zare and P. Gader, "Pattern recognition using functions of multiple instances," *Proceedings of the International Conference on Pattern Recognition*, pp. 1092–1095, Aug. 2010.

[9] A. M. Fuller, *Investigation of select energetic materials by differential reflection spectrometry*, Ph.D. dissertation, University of Florida, Department of Materials Science and Engineering, 2007.

[10] R. E. Hummel, A. M. Fuller, C. Schollhrn, and P. H. Holloway, "Detection of explosive materials by differential reflection spectroscopy," *Applied Physics Letters*, vol. 88, no. 231903, pp. 898–910, June 2006.